

Electronic Supplementary Information (ESI)

Graphene/Rh-Complex Hydrogel for Boosting Redox Biocatalysis

Joon Seok Lee,^a Sahng Ha Lee,^a Jangbae Kim,^b and Chan Beum Park ^{*a}

^aDepartment of Materials Science and Engineering, Korea Advanced Institute of Science and Technology (KAIST), 335 Science Road, Daejeon 305-701, Korea, ^bBattery R&D, LG Chem, Ltd. 104-1, Moonjido, Yuseong-gu, Daejeon, 305-380, Korea

Experimental Section

Materials: Graphite powder was obtained from Kropfuhl AG (Germany). $[\text{Cp}^*\text{Rh}(\text{phen})\text{Cl}]^+$ and $[\text{Cp}^*\text{Rh}(\text{bpy})\text{Cl}]^+$ were synthesized according to the literature.¹⁻³ All other chemicals were purchased from Sigma Aldrich (St. Louis, MO) in an analytical reagent grade and used without further purification.

Synthesis of the graphene/Rh-complex hydrogel: The graphene hydrogel was prepared by a one-step hydrothermal reduction of graphene oxide (GO).⁴ Briefly, GO was obtained by the oxidation of natural graphite powder. We dissolved GO in an aqueous solution to make 2 mg/mL, sealed the solution in a Teflon-lined autoclave, and maintained it at 200 °C. After incubation for 14 h, the autoclave was naturally cooled down to room temperature. The graphene/Rh-complex hydrogel was prepared by immersing the graphene hydrogel in a Rh complex solution, followed by incubation for 12 h under shaking. The resulting hydrogel was washed rigorously with deionized water to remove any unbound Rh complex until no release of Rh complex into the supernatant, which was verified by UV/Vis spectroscopic analysis. To estimate the amount of Rh complex loaded in the graphene hydrogel, the amount of unbounded Rh complex in the supernatant was measured spectrophotometrically from its absorbance at 275 nm using calibration curves (**Figure S13**). From the amounts of the Rh complex initially dissolved in solution and

the unbound Rh complex after incubation, the amount of Rh complex loaded on freeze-dried graphene hydrogel was estimated to be approximately 20 nmol/mg. We prepared *colloidal* graphene/Rh-complex sheets by grinding the freeze-dried graphene/Rh-complex hydrogel and re-dispersing them in deionized water (**Figure S7A**). The initial turnover frequency was calculated as the moles of NADH generated during the first 20 minutes per mole of Rh complex.^{1,5,6}

Electrochemical regeneration of cofactor and enzymatic synthesis of L-glutamate: The freeze-dried graphene/Rh-complex hydrogel (5 mg), a freeze-dried pristine graphene hydrogel alone (5 mg), or a porous carbon felt (5 mg) was connected to carbon wires that were used as a working electrode with carbon paste. A single-compartment cell was configured with three electrodes: the graphene/Rh-complex hydrogel (working), a platinum wire (counter), and an Ag/AgCl (reference, 0.197 V versus normal hydrogen electrode) connected to a potentiostat/galvanostat (EG&G, Model 273A, Korea). For the NADH regeneration experiment, 10 mL of phosphate buffer (0.1 M, pH 7.0) containing 1 mM NAD⁺ was stirred at 200 rpm in the electrochemical cell with 5 mg graphene/Rh-complex hydrogel and the potential was applied at – 0.8 V versus Ag/AgCl. To test the catalytic activity of *free* Rh complex and *colloidal* graphene/Rh-complex sheets, we used 10 µM of *free* Rh complex (i.e., 100 nmol in 10 mL buffer) and *colloidal* graphene/Rh-complex sheets (5 mg in 10 mL buffer), respectively, with 5 mg carbon felt as a working electrode. The concentration of NADH was measured spectrophotometrically from its absorbance at 340 nm using a V-650 spectrophotometer (JASCO Co., Japan). The reaction solution for the enzymatic synthesis of L-glutamate consisted of NAD⁺ (1 mM), α-ketoglutarate (10 mM), ammonium sulfate (100 mM), and glutamate dehydrogenase (GDH, 40 U), based on a phosphate buffer (0.1 M, pH 7.0), with the graphene/Rh-complex hydrogel (0.5 mg ml⁻¹). High performance liquid chromatography (LC-20A prominence, Shimadzu Co., Japan), equipped with an Inertsil C18 column (ODS-3V, length, 150 mm), was used for the analysis of enzymatic reactions in the graphene hydrogel system. Samples were eluted by phosphoric acid solution (0.085%) at a flow rate of 1.0 ml/min and detected at 210 nm.

Characterization: The morphology of the graphene/Rh-complex hydrogel was observed using an S-4800 field emission scanning electron microscope (Hitachi High-Technologies CO., Japan). and a Tecnai F20 TEM (Philips, Japan) operating at 200 kV. The BET surface area of the graphene/Rh-complex hydrogel was measured using a Micromeritics TriStar II (Micromeritics, Norcross, GA) with N₂ gas as the adsorbate at 77.3 K. The Rh complex immobilized in the graphene hydrogel was analyzed through the measurement of its XPS spectra using a JPS-9000MX spectrometer (JEOL Ltd., Japan). The surface charges of the pristine graphene dispersion and Rh complex/graphene dispersion in water at pH 7.0 were investigated by zeta-potential measurements (Photal Otsuka ELS-Z, Japan). To sweep the potential in cyclic voltammograms, a pristine graphene hydrogel and a graphene/Rh-complex hydrogel were sliced and deposited on a GC disk. A single-compartment cell was configured with three electrodes: a GC disk (working, 0.03 cm²), a platinum wire (counter), and an Ag/AgCl (reference, 0.197 V versus normal hydrogen electrode) connected to a potentiostat/galvanostat (Model 273A, EG&G, Princeton, NJ). The FTIR spectra of graphene oxide and the graphen/Rh-complex hydrogel were obtained using a FTIR 200 spectrophotometer (Jasco Co., Japan). ¹H NMR spectra of Rh(phen) complex and Rh(bpy) complex were recorded using a Bruker Avance 400 spectrometer (Bruker, Billerica, MA).

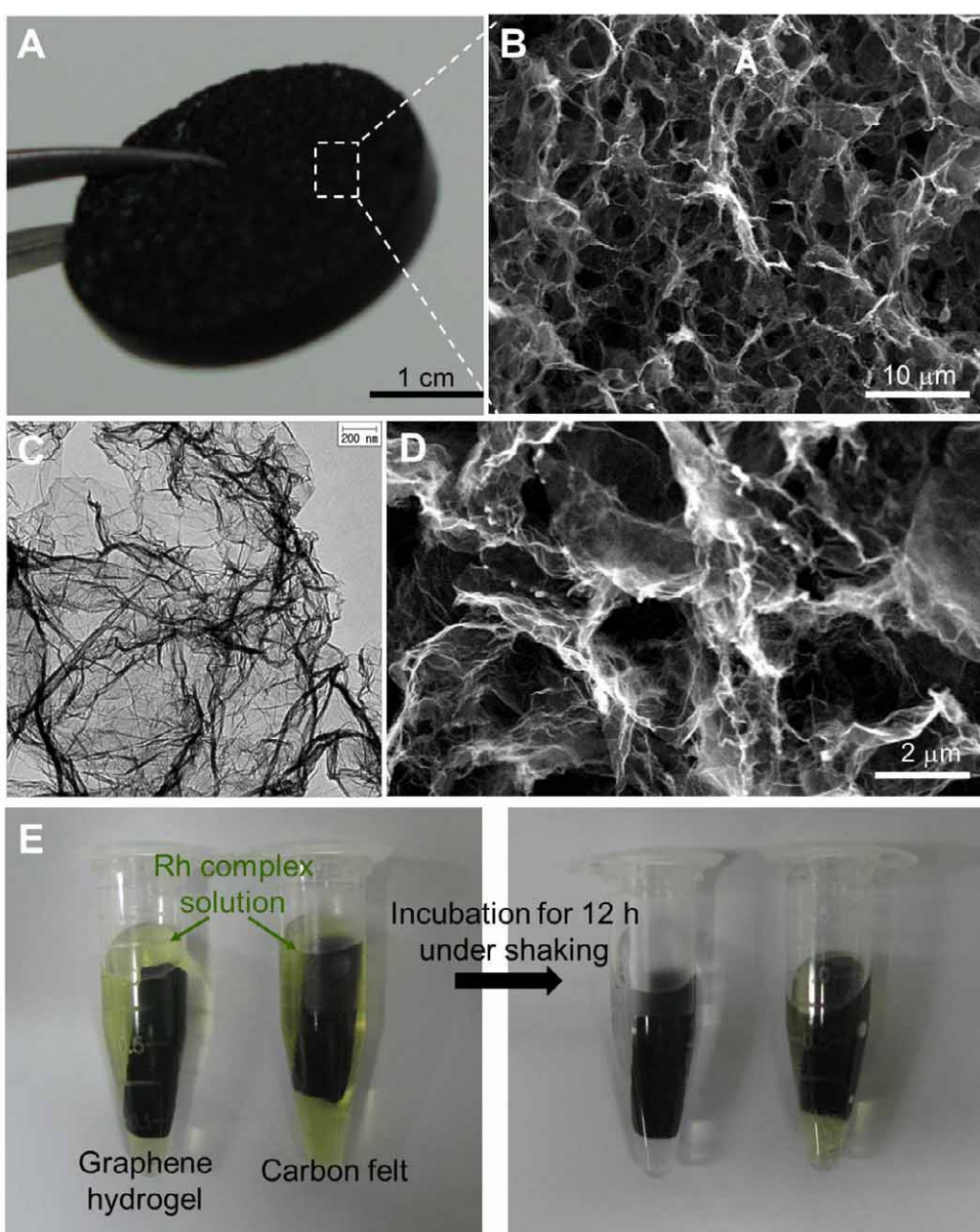


Figure S1. (A) Photograph, (B,D) SEM, and (C) TEM images of the graphene/Rh-complex hydrogel. (E) Photograph images taken before/after 12 h incubation of graphene hydrogel and carbon felt in Rh(phen) complex solutions, respectively. The Rh complex solution became clear after incubation with the graphene hydrogel. In case of the carbon felt, there was no change in the color of the Rh complex solution, which indicates no adsorption of Rh complex on the carbon felt.

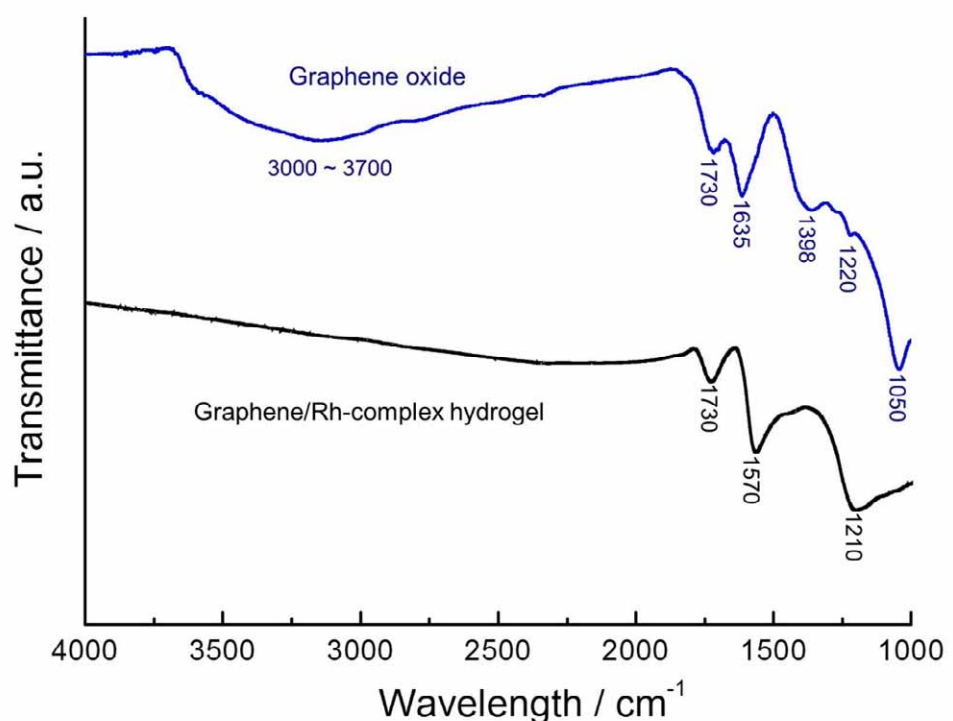


Figure S2. FT-IR spectra of graphene oxide and graphene/Rh-complex hydrogel. The carbonyl moieties at 1730 cm^{-1} still existed on the graphene surface after the reduction of graphene oxide, which should bind positively charged Rh complex to the graphene hydrogel through an electrostatic interaction.

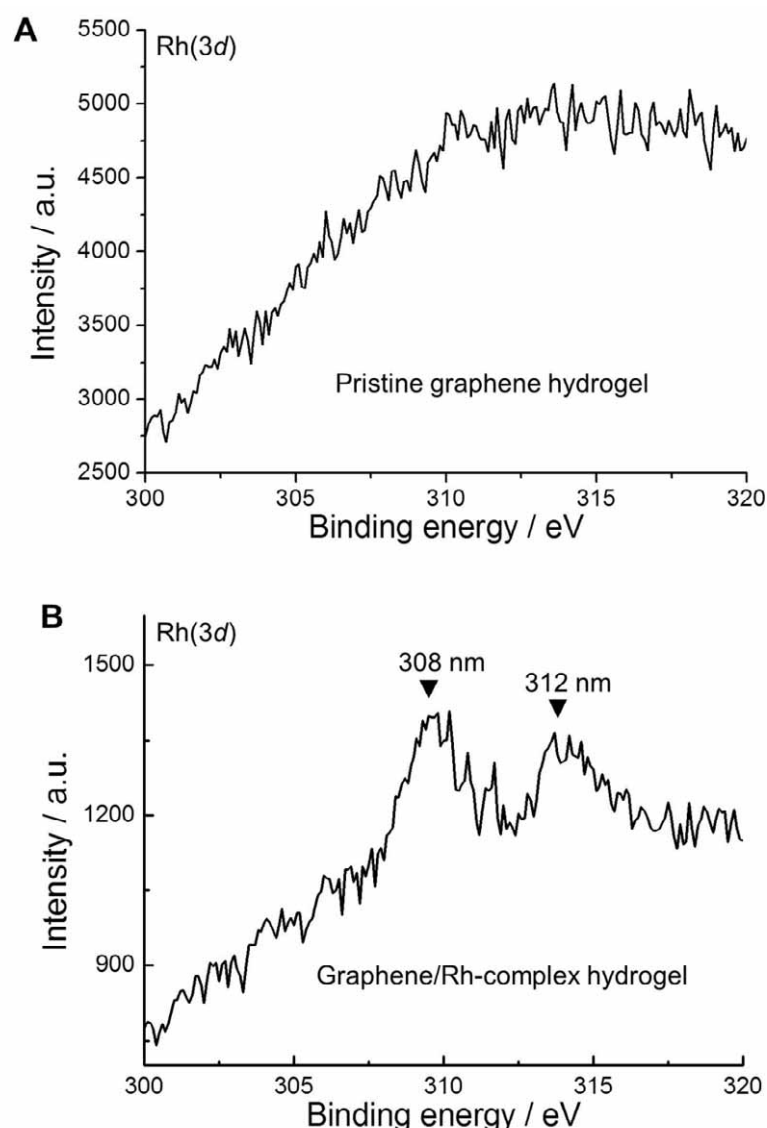


Figure S3. X-ray photoelectron spectroscopy (XPS) spectra of (A) pristine graphene hydrogel and (B) graphene/Rh-complex hydrogel. The peaks at 308 and 312 eV in the Rh 3d XPS profile of the graphene/Rh-complex hydrogel are characteristic peaks of Rh 3d_{5/2} and Rh 3d_{3/2} of Rh complex, respectively.

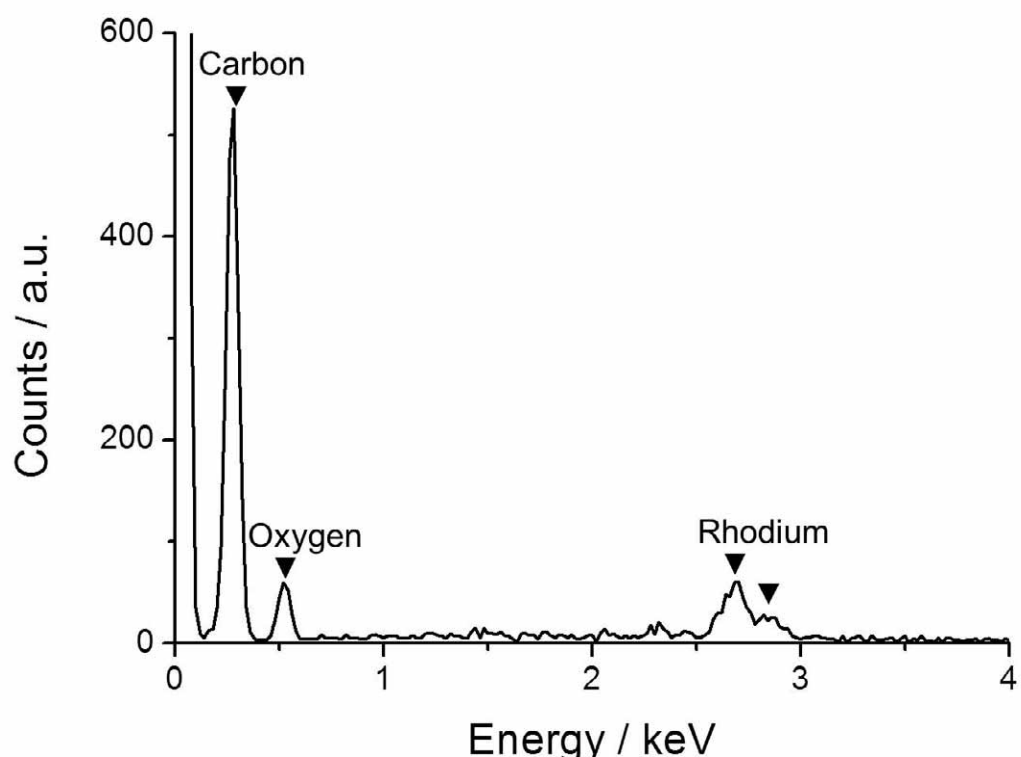


Figure S4. Energy dispersive X-ray (EDX) spectrum of graphene/Rh-complex hydrogel. The EDX spectrum shows the presence of Rh element in the graphene/Rh-complex hydrogel.

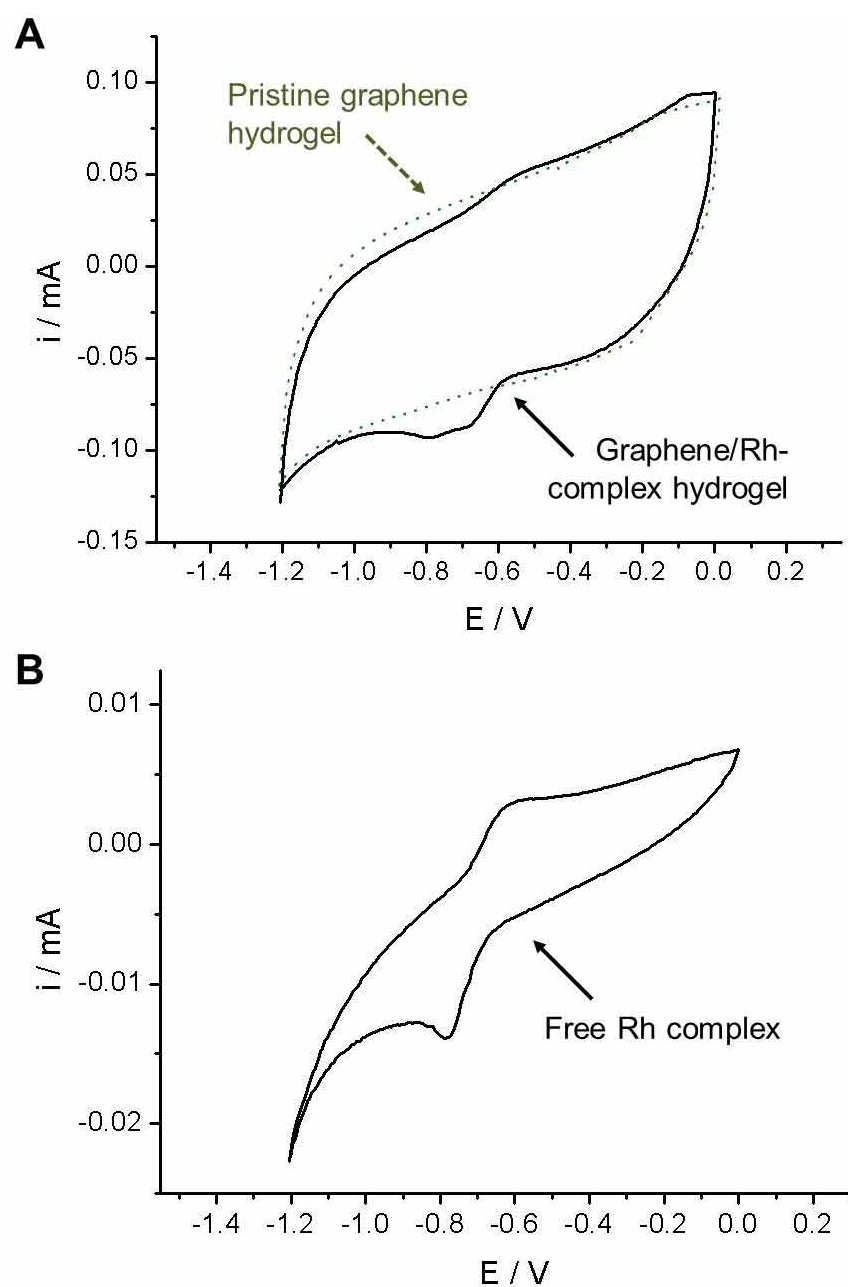


Figure S5. Cyclic voltammograms for (A) pristine graphene hydrogel and graphene/Rh-complex hydrogel deposited on a GC electrode, respectively, and (B) free Rh complex in a phosphate buffer solution (100 mM, pH 7.4). The scan rate was 50 mVs⁻¹. A reduction peak potential at approximately -0.75 V for the graphene/Rh-complex hydrogel is similar to that of free Rh complex dissolved in a buffer solution.

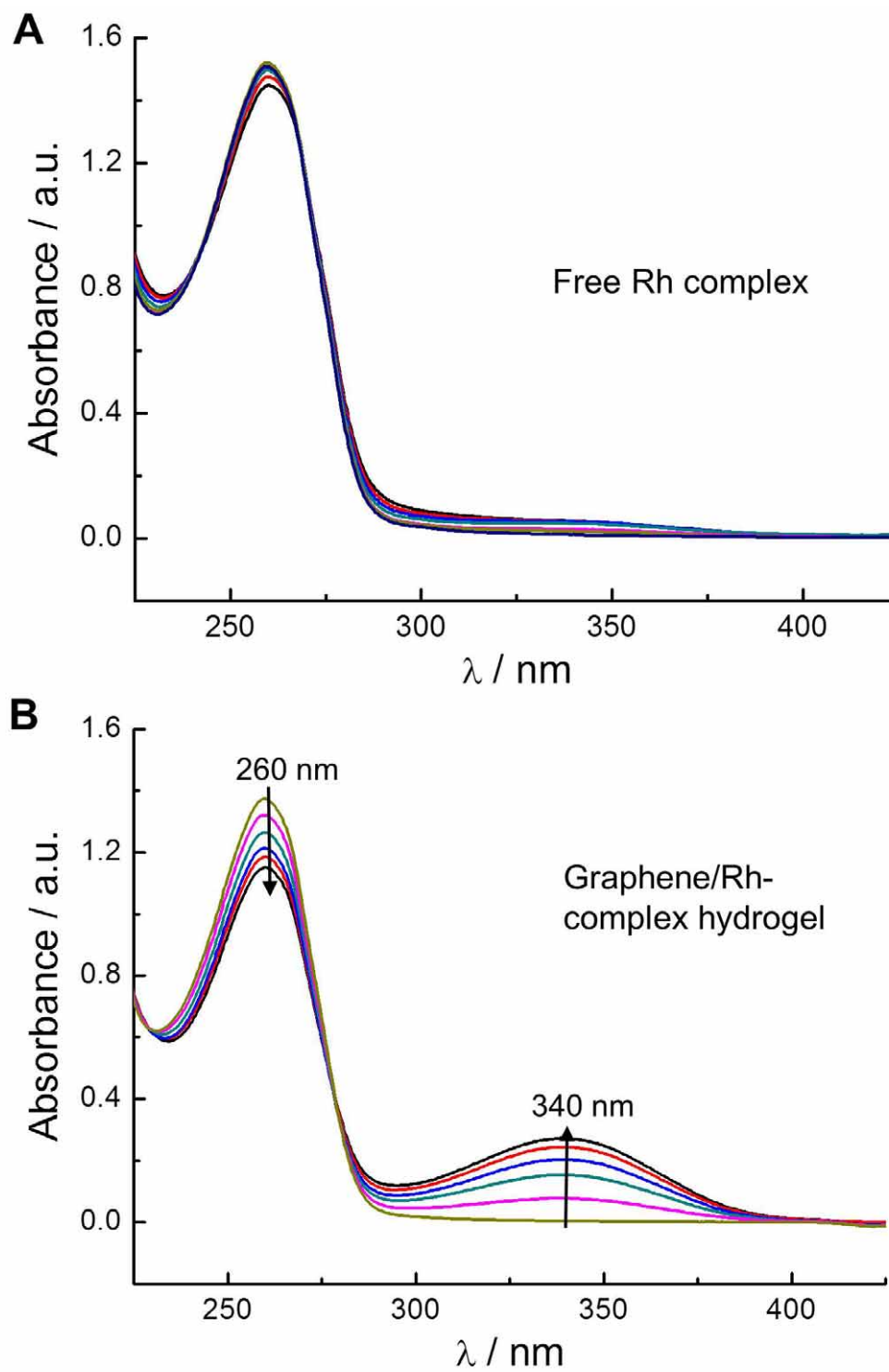


Figure S6. Spectral measurement of the concentration of NADH regenerated from NAD^+ with (A) free Rh complex and (B) graphene/Rh-complex hydrogel. The absorption change at 260 and 340 nm were correlated with gradual regeneration of NADH.

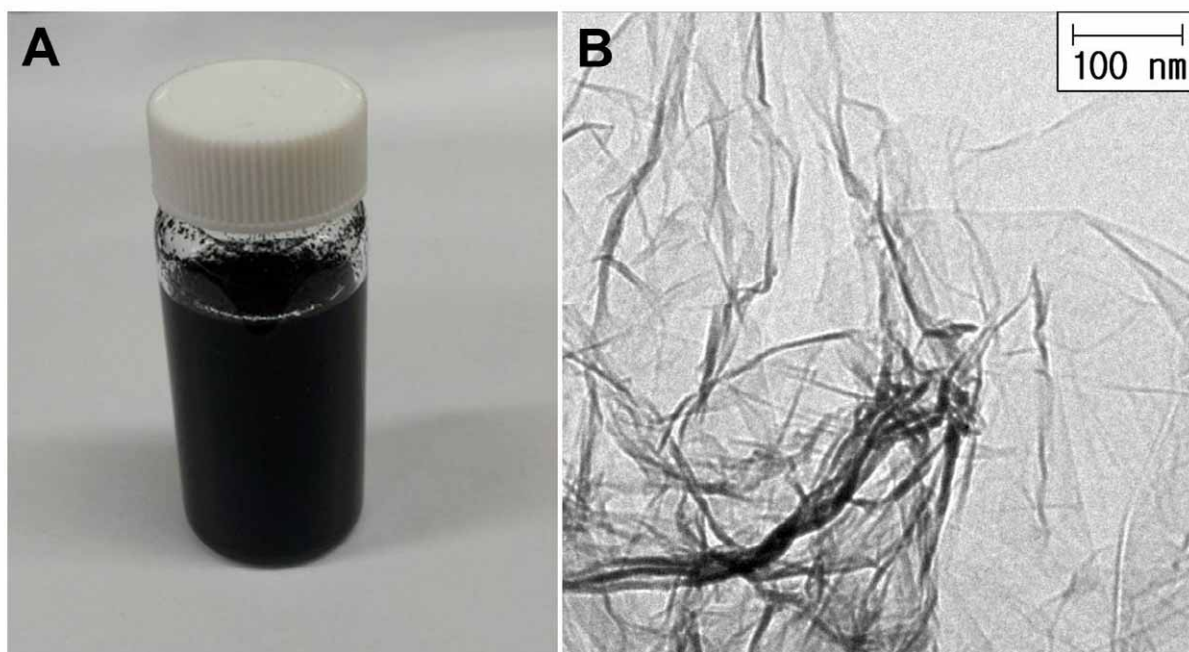


Figure S7. (A) Photograph of a solution containing colloidal graphene/Rh-complex sheets and (B) their TEM image. The micro-particulate graphene/Rh-complex was obtained by grinding freeze-dried graphene/Rh-complex hydrogel.

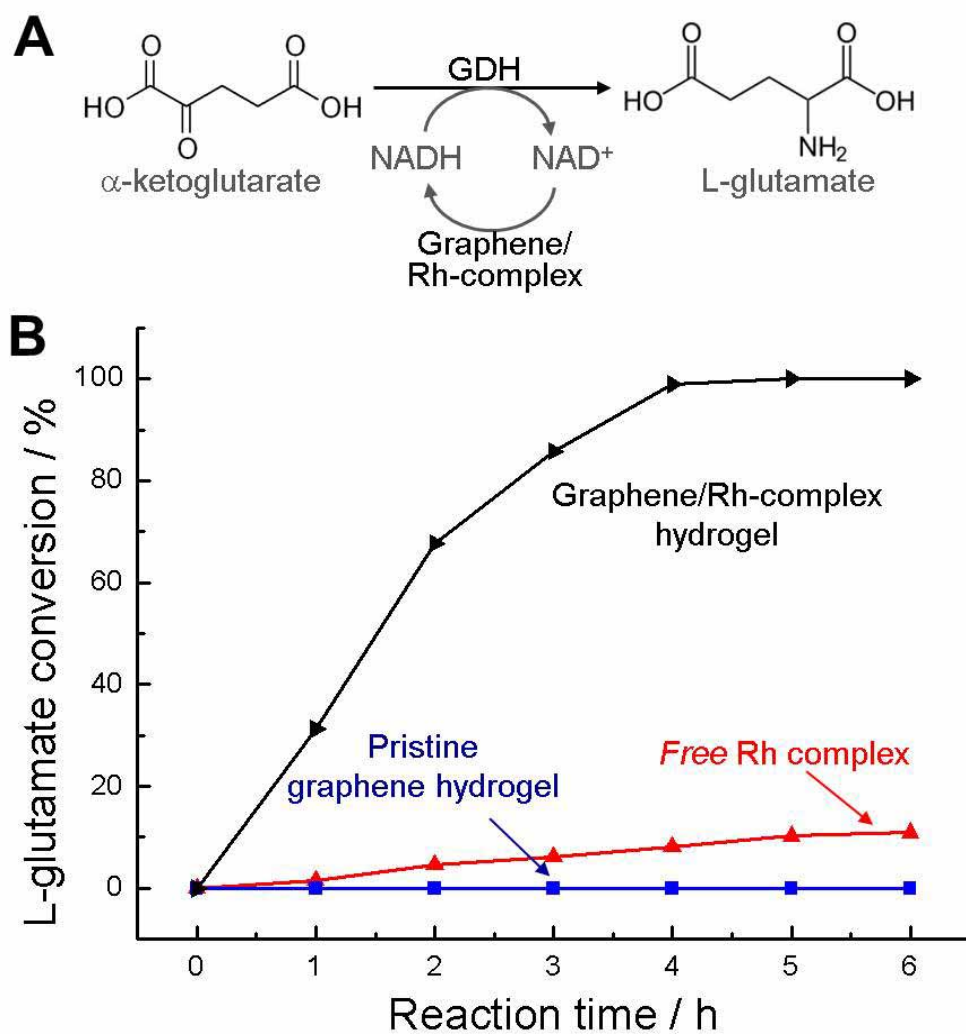
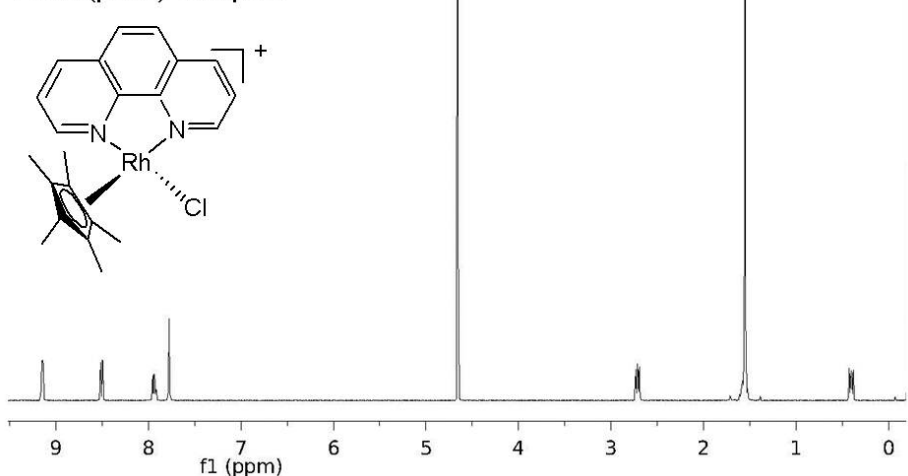


Figure S8. (A) A scheme for the enzymatic synthesis of L-glutamate driven by L-glutamate dehydrogenase (GDH) through electrochemical cofactor regeneration. (B) Time profiles for L-glutamate conversion in three different reduction systems: (1) graphene/Rh-complex hydrogel, (2) pristine graphene hydrogel only, and (3) free Rh complex. The initial concentration of α -ketoglutarate was 10 mM.

A. Rh(phen) complex



B. Rh(bpy) complex

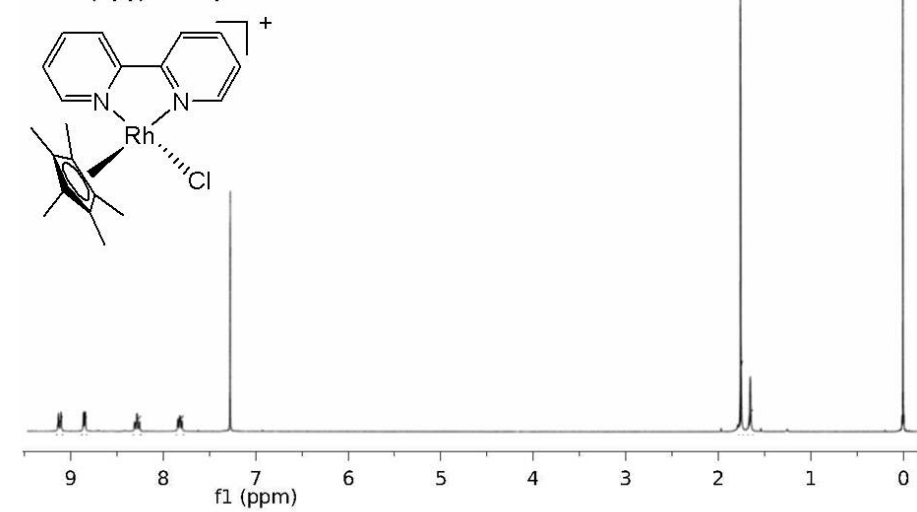


Figure S9. NMR spectra of Rh(phen) complex and Rh(bpy) complex. (A) Rh(phen) complex: ¹H NMR (400 MHz, D₂O): δ =9.3 (d, 2H; H-3,3'), 8.7 (d, 2H; H-6,6'), 7.90-7.95 (t, 2H; H-5,5'), 7.75 (t, 2H; H-4,4'), 1.65 ppm (s, 15H, Cp*). (B) Rh(bpy) complex: ¹H NMR (400 MHz, D₂O): δ =9.11 (d, 2H; H-3,3'), 8.84 (d, 2H; H-6,6'), 8.27 (t, 2H; H-5,5'), 7.81 (t, 2H; H-4,4'), 1.75 ppm (s, 15H, Cp*).

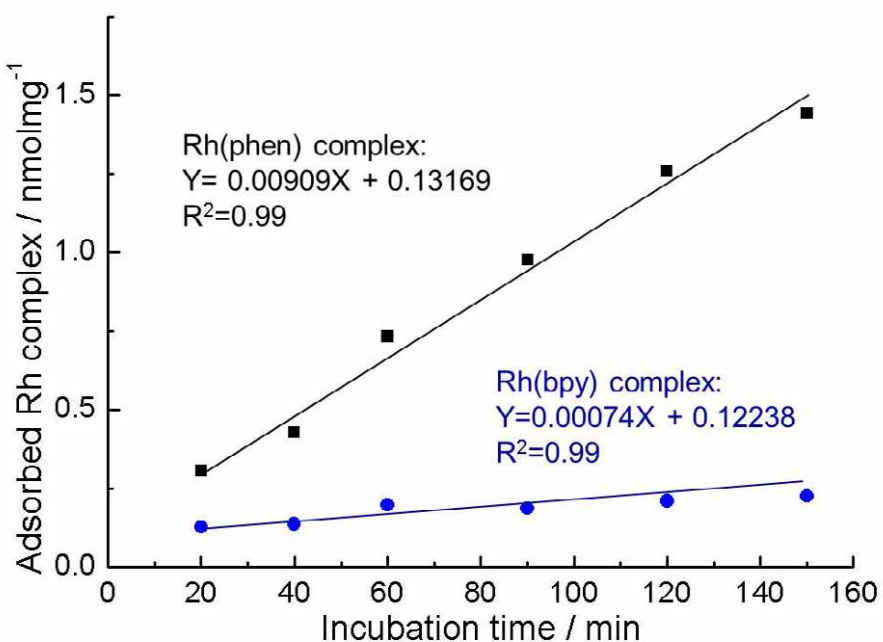


Figure S10. The adsorption of Rh(phen) complex and Rh(bpy) complex to the graphene hydrogel in each respective Rh-complex solution (3 μ M) during initial 150 min of incubation. The linear time profile of the adsorption at initial incubation time was fitted for the determination of adsorption rate according to the following equations: black line [Rh(phen) complex]: $Y=0.00909X+0.13169$, $R^2=0.99$, blue line [Rh(bpy) complex]: $Y=0.00074X+0.12238$, $R^2=0.99$.

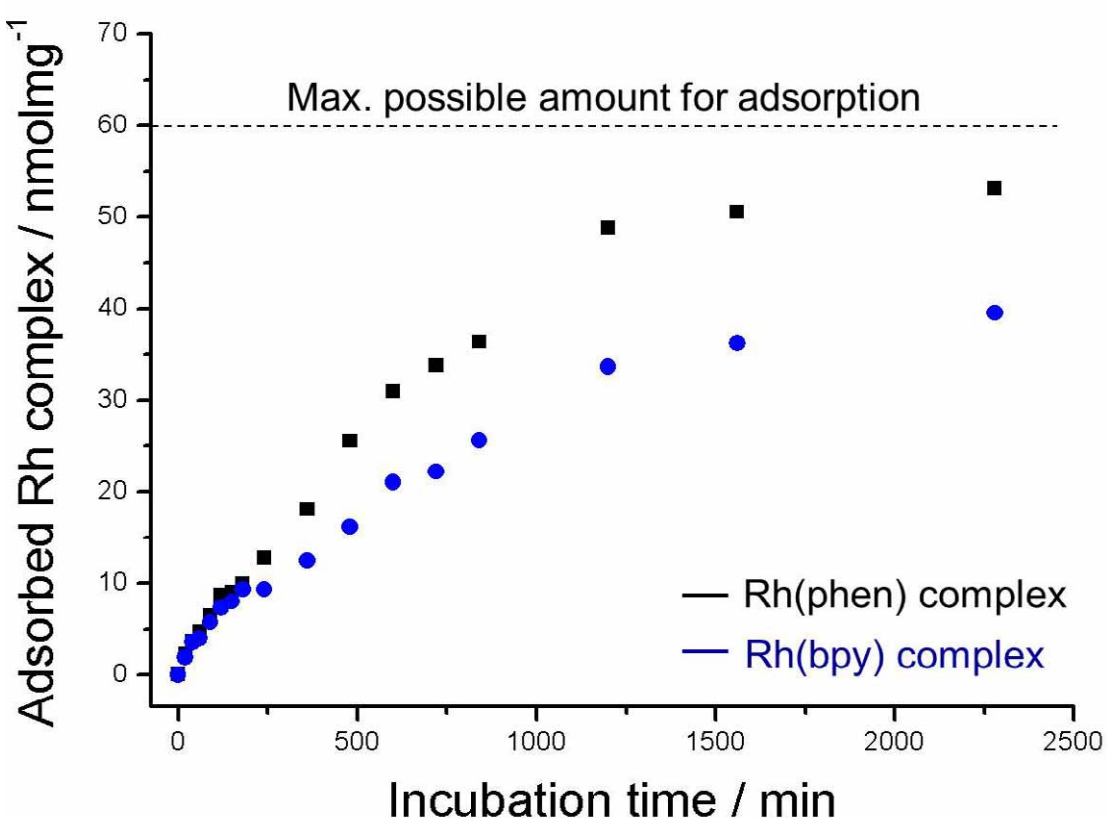


Figure S11. Time profiles for the adsorption of the Rh(phen) complex and Rh(bpy) complex to the graphene hydrogel in each respective solution containing 100 μM Rh-complex. The amount of Rh(phen) complex and Rh(bpy) complex adsorbed in the graphene hydrogel were approximately 88% and 61% of the maximum possible adsorption amount (i.e., 60 nmol Rh complex per mg graphene), respectively, after 20 h incubation.

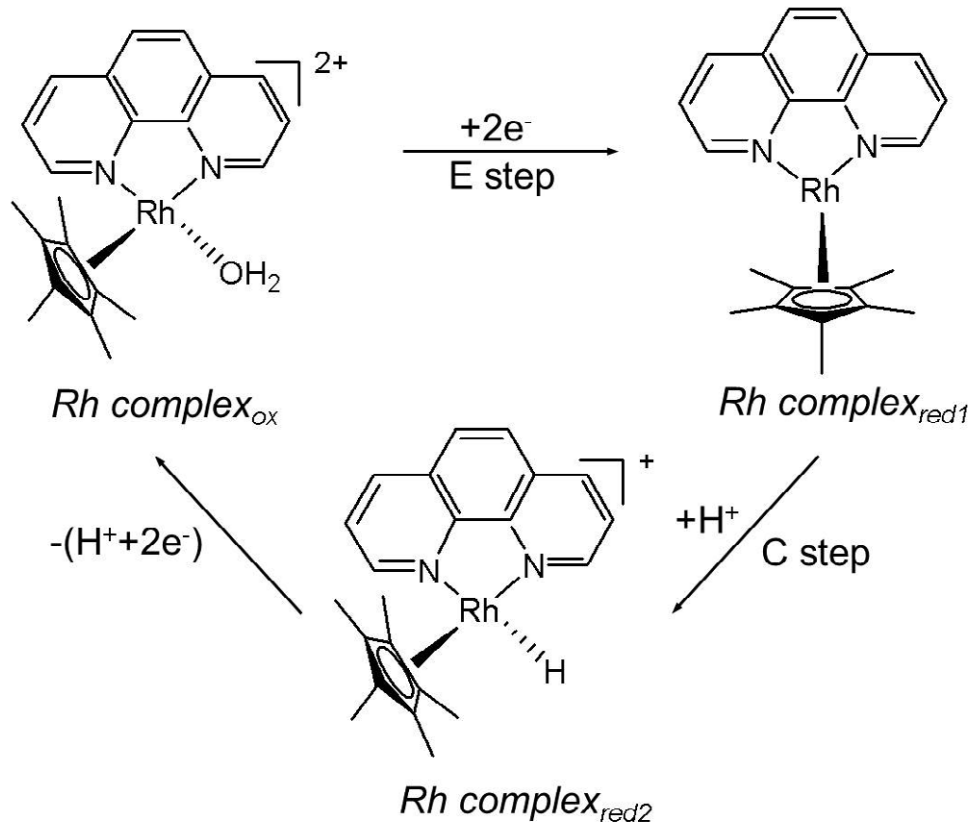


Figure S12. Molecular structures of three different electrochemical states of Rh(phen) complex. The active reduced form $\text{Rh(phen) complex}_{\text{red2}}$ is generated through a typical electrochemical/chemical (EC process).^{1,7} The $\text{Rh complex}_{\text{ox}}$ is reduced to the first reduced form ($\text{Rh complex}_{\text{red1}}$) by taking two electrons from the electrode during the E step, which neutralizes the overall net charge of $\text{Rh complex}_{\text{red1}}$. Then, the $\text{Rh complex}_{\text{red1}}$ is chemically reduced into $\text{Rh complex}_{\text{red2}}$ (C step). NAD(P)H is regenerated from NAD(P)^+ through interactions with the active form ($\text{Rh complex}_{\text{red2}}$) by accepting one proton and two electrons from the $\text{Rh complex}_{\text{red2}}$ that returns to the $\text{Rh complex}_{\text{ox}}$.

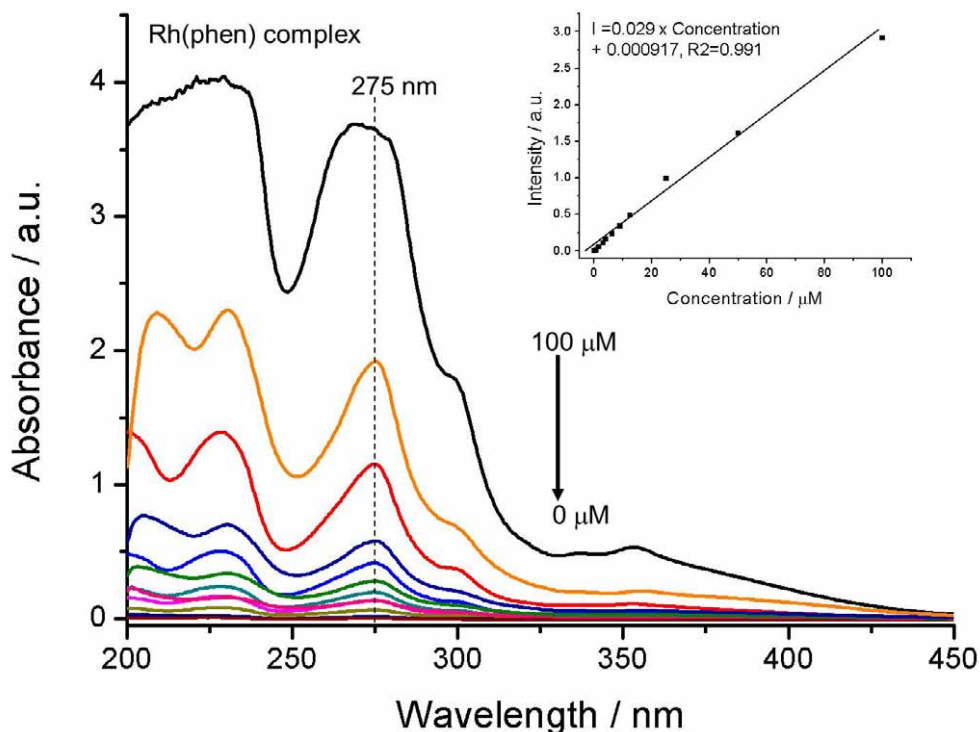


Figure S13. Absorbance spectra of Rh(phen) complex at different concentration (0~100 μM). Inset: calibration curve corresponding to the absorbance at $\lambda = 275$ nm of the Rh(phen) complex.

Reference for the Supporting Information

- 1 F. Hollmann, A. Schmid, E. Steckhan, *Angew. Chem. Int. Ed.*, 2001, **40**, 169.
- 2 F. Hildebrand, C. Kohlmann, A. Franz, S. Lutz, *Adv. Synth. Catal.*, 2008, **350**, 909.
- 3 J. Gajdzik, J. Lenz, H. Natter, A. Walcarius, G. W. Kohring, F. Giffhorn, M. Gollu, A. S. Demir, R. Hempelmann, *J. Elecrochem. Soc.*, 2012, **159**, F10.
- 4 Y. Xu, K. Sheng, C. Li, G. Shi, *ACS Nano*, 2010, **4**, 4324
- 5 F. Hollmann, I. W. C. E. Arends, K. Buehler, *ChemCatChem*, 2010, **2**, 762.
- 6 E. Steckhan, S. Herrmann, R. Ruppert, J. Thommes, C. Wandrey, *Angew. Chem. Int. Ed.*, 1990, **29**, 388.
- 7 H.-K. Song, S. H. Lee, K. Won, J. H. Park, J. K. Kim, H. Lee, S.-J. Moon, D. K. Kim, C. B. Park, *Angew. Chem. Int. Ed.*, 2008, **47**, 1749.